Mechanistic Study on the Synthesis of a Porous Zincosilicate VPI-7 Containing Three-Membered Rings

ARTICLE *in* THE JOURNAL OF PHYSICAL CHEMISTRY C · DECEMBER 2010

Impact Factor: 4.77 · DOI: 10.1021/jp109373z

6 AUTHORS, INCLUDING:

Shinji Kohara
Japan Synchrotron Radiation Research Ins…

247 PUBLICATIONS **2,469** CITATIONS

SEE PROFILE

Mechanistic Study on the Synthesis of a Porous Zincosilicate VPI-7 Containing Three-Membered Rings

Yasuhiro Suzuki,[†] Toru Wakihara,[||,†] Shinji Kohara,[‡] Keiji Itabashi,[†] Masaru Ogura,[§,†] and Tatsuya Okubo*[,†]

Department of Chemical System Engineering, The University of Tokyo, 7-3-1 Hongo, Bunkyo-ku, Tokyo 113-8656, Japan, and Japan Synchrotron Radiation Research Institute, 1-1-1 Kouto, Sayo, Hyogo 679-5198, Japan

Received: September 30, 2010; Revised Manuscript Received: November 18, 2010

Changes in the medium-range order during the crystallization of VPI-7, a zincosilicate zeolite containing 3-membered rings (3Rs), were characterized by high-energy X-ray diffraction and Raman spectroscopy. Distinct changes in the medium-range order have been observed, especially due to the formation of 3Rs in the initial stages of the crystallization of VPI-7. Increases in the formation of other rings during crystallization have also been confirmed. Addition of Zn has been shown to promotion of the formation of 3Rs in these amorphous solids.

Introduction

Zeolites are hydrated, crystalline tectoaluminosilicates that are constructed from TO_4 tetrahedra (T = Si, P, Al, Zn, Ge, etc.).[1,2] Their structures contain nanometer-sized and well-ordered void spaces. So far, 194 kinds of zeolite structures have been authorized and many mechanistic studies on zeolites have been made.[3–5] As a result, the possibility of tuning framework structures and pore dimensions has made zeolites the most successful materials for various applications such as gas adsorption and catalysis. It is known that introduction of 3-membered rings (3R: ring structures are denoted *n*R, where *n* is the number of oxygen atoms in the ring) is one way to promote the formation of extra-large pores.[6–9] Because of the desirability of large pores, extensive efforts have been made into the synthesis of zeolites containing 3Rs in their structures; however only 15 zeolite structures containing 3Rs have been authorized out of 194 structures.[10] This comes from the lack of control in the changes in the atomic arrangement as the samples change from amorphous to crystalline states. VPI-7 (structure type: VSV), the first zincosilicate zeolite containing 3R,[11,12] is the target of this study. Figure 1 shows the structure and ring distribution of VPI-7. The VPI-7 framework consists of 3, 4, and 5-membered rings (3R, 4R, and 5R, respectively) assembled in three dimensions to produce larger units such as 8- and 9-membered rings (8R and 9R). Figure 1 also shows the average distances of the second nearest neighbor of T−O, O−O, and T−T and the third nearest neighbor of T−O, indicating that these distances are generally shorter in smaller rings than comparable distances in larger rings. By characterizing the distances of the second-nearest neighbor or longer correlations to address medium-range order in the crystalline material and/or amorphous solid prior to zeolite crystallization, the transitions from the amorphous to the crystalline state will be better understood.[13–15] To extract the information on the ring structures present in the amorphous solid, many studies have used Raman

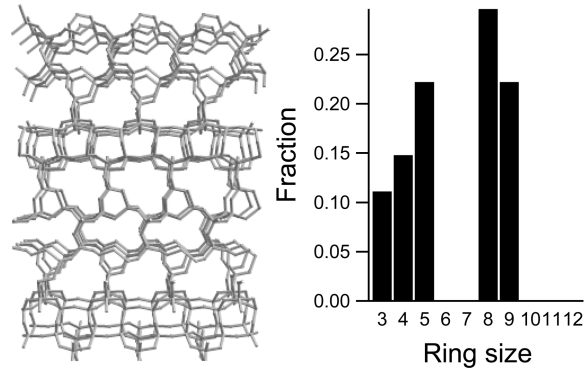

	3R	4R	5R	8R	9R
T-O (2nd)	3.40	3.79	3.77	4.22	4.14
O-O (2nd)	–	3.95	4.14	4.61	4.74
T-T (2nd)	–	4.21	4.69	5.67	5.55
T-O (3rd)	–	–	4.63	5.78	5.95

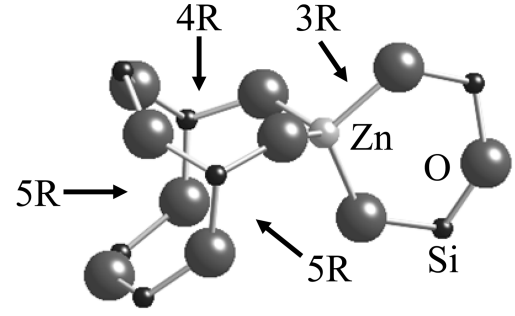

Figure 1. Top left: the crystal structure of VPI-7.[12] Top right: the ring distribution of VPI-7 present in the three-dimensional configurations. Middle: a table containing the average distances (Å) of the second nearest neighbors of T−O, O−O, and T−T and the third T−O (T = Si or Zn). Note that other correlations, such as the third T−T and O−O, are longer than 5.9 Å. Bottom: a shape of smaller ring structures present in VPI-7.

* Corresponding author. Telephone: +81-3-5841-7348. Fax: +81-5800-3806. E-mail: okubo@chemsys.t.u-tokyo.ac.jp.
[†] The University of Tokyo.
[‡] Japan Synchrotron Radiation Research Institute.
[§] Present address: Institute of Industrial Science, The University of Tokyo, 4-6-1 Komaba, Meguro-ku, Tokyo 153-8505, Japan.
[||] Present address: Department of Environmental and Information Sciences, Yokohama National University, 79-7 Tokiwadai, Hodogaya-ku, Yokohama 240-8501, Japan.

10.1021/jp109373z
Published on Web 12/20/2010

spectroscopy.[16–18] It is now also possible to analyze the structure of disordered materials using the third generation synchrotron radiation sources,[13–15,19] using high-energy X-ray diffraction (HEXRD) measurements. Recently, Wakihara et al.[13–15] have reported the application of the HEXRD technique to determine the structure of the amorphous solid obtained during crystallization of ZSM-5, zeolite A and X. The changes in the atomic arrangement during the changes from the amorphous to the crystalline VPI-7 is also of interest. To the best of our knowledge, there are no reports on the crystallization mechanism of zincosilicate zeolites including VPI-7. In this study, VPI-7 has been synthesized and the changes in the atomic arrangement from amorphous to crystalline phases have been characterized by a combination of HEXRD and Raman spectroscopy.

Experimental Section

The noncrystalline zincosilicate gels were prepared by conventional methods without organic structure-directing agents. Sodium hydroxide pellets (96% NaOH; Wako Pure Chemical Industries, Ltd.) were dissolved in a small amount of distilled water, to keep the mixture sufficiently alkaline to dissolve zinc oxide. Next, zinc oxide (99.999% ZnO; Sigma-Aldrich, Inc.) was added to the solution resulting in a milky solution. Additional distilled water was added up to the total amount described below, and the solution was stirred for 30 min. Finally, fumed silica, Cab-O-Sil M5 (Cabot Corp.), which was assumed to be 100% SiO_2, was added to the solution as a silica source. The solution was distributed into several 23 mL Teflon-lined stainless-steel autoclaves. The optimized batch composition was $0.44Na_2O{:}0.13ZnO{:}SiO_2{:}44H_2O$, and each weight of reactants in one autoclave was as follows: 0.587 g of sodium hydroxide, 0.176 g of zinc oxide, 1.000 g of SiO_2, and 13.20 g of distilled water. The autoclaves were put into convection oven that can rotate the autoclaves, and heated at 20 rpm under autogenous pressure at 448 K for 1, 12, 18, 31, and 120 h, designated as V1, V12, V18, V31, and V120, respectively. After the prescribed periods of heating, the recovered solid products were washed with distilled water, and vacuum-dried at room temperature. The phases present in the products were identified by conventional X-ray diffractometry (XRD: Mac Science MO3XHF,[22] Tokyo Japan) using Cu Kα radiation operated at 50 kV and 300 mA. Samples recovered after the hydrothermal treatments were used for HEXRD and Raman spectroscopic measurements. Amorphous zincosilicates from different batch compositions were prepared as shown in the Supporting Information to reveal the effect of zinc addition on the structure of the amorphous network. Furthermore, amorphous aluminosilicates for the synthesis of ferrierite and sodalite were also prepared as shown in the Supporting Information and their network structures were compared with amorphous zincosilicate.

High-energy X-ray diffraction experiments were carried out on a horizontal two-axis diffractometer, optimized for structural measurements in glass and liquid, built at the BL04B2 high-energy monochromatic bending magnet beamline of SPring-8. A bent Si(220) crystal mounted on the monochromator stage fixed at a Bragg angle of 3° in the horizontal plane, provides an incident photon energy of 61.63 keV (Wavelength: 0.2012 Å). Pelletized samples were fixed to the sample stage. Q_{max} collected in this study is 25 $Å^{-1}$. The collected data were subjected to well established analysis procedures including absorption, background and the Compton scattering corrections followed by normalization to the Faber-Ziman total structure factor, $S(Q)$.[20] The pair distribution function, $G(r)$, is derived from eq 1,

$$G(r) = 4\pi r[\rho(r) - \rho_0] = \frac{2}{\pi}\int_{Q_{min}}^{Q_{max}} \{Q[S(Q) - 1]\sin(Qr)\}\, dQ \quad (1)$$

where $\rho(r)$ is the microscopic pair density and ρ_0 is the average number density.[21] Note that the compositions of all samples were measured using an inductively coupled plasma atomic emission spectrometer (ICP-AES: P-4010, Hitachi Ltd., Tokyo, Japan) and no significant changes were seen in the Si/Zn ratios (ca. 1.60) throughout the treatments. Therefore, the $G(r)$ values are calculated using the same composition of Si:Zn:O:Na = 1.6:1.0:5.2:2.0.

Raman spectroscopy can be employed to characterize the ring statistics for the elucidation of the crystallization process of VPI-7. Raman spectra were obtained using a Raman spectrometer (JASCO Corp., NRS-1000) equipped with green laser (532 nm). Raman spectra were recorded over the range 300 and 800 cm^{-1}, and integrated for 30 s at least twice, or more for samples with weak scattering. For this measurement, samples were dried again to remove residual water.

Results and Discussion

Powder XRD patterns of the samples are shown in Figure 2. Slight Bragg peaks are observed in the sample obtained by heating for 18 h (V18), while no such peaks are seen in the samples obtained by heating for 1 and 12 h (V1 and V12, respectively). Therefore, it is concluded that nucleation of VPI-7 has occurred between 12 and 18 h into the hydrothermal synthesis. The crystallization was confirmed to be complete after 120 h (V120). To extract quantitative information from the HEXRD regarding the atomic arrangements in the amorphous and/or crystalline materials, the pair distribution functions, $G(r)$, were calculated by the Fourier transformation of the total structure factor, $S(Q)$.

Figure 3 shows the $G(r)$ of products for the synthesis of VPI-7. From these $G(r)$, it is possible to identify the various distances associated with a number of features by correlating them with the calculated $G(r)$ using PDF-gui[22] as shown in Figure 4. The first three peaks at 1.6, 2.0, and 2.6 Å in the $G(r)$ curves are related to the Si−O, Zn−O, and O−[Si]−O correlation lengths, respectively. The distinct feature seen around 3.1 Å is due to both Si−Si(Zn) and O−Zn−O correlation lengths. All of these lengths are similar in all the possible ring structures and hence cannot provide any specific information to help identify the type of ring structures present in the amorphous solid. The peaks in the $G(r)$ show that differences in the ring structures only appear beyond 3.3 Å. Correlation of the second nearest neighbor of T−O (T: tetrahedral atoms, in these cases, Si and Zn) in 3R is around 3.3 Å which appears as a tail of the peak of 3.1 Å and this tail peak is slightly less pronounced as the synthesis continues. The peak at ca. 3.7 Å, which is mainly due to the second nearest neighbor of T-O in 4R and 5R (See Figure 1), is more pronounced as the synthesis progresses; indicating the fraction of 4 and 5R increases during crystallization. Similarly, the peak at ca. 4.1 Å is also more pronounced with further crystallization, and is mainly due to the second nearest neighbor of T-O in 8R and 9R as shown in Figures 1 and 4. These results show that the fraction of 3R decreases and other rings increase as the synthesis progresses.

To confirm the Zn addition has an effect on the formation of 3R, Figure 5 shows the $G(r)$ of the samples obtained by extracting the amorphous zincosilicate solids with batch compositions of Si/Zn = 7.7, 20, 200, and ∞. Comparison of the different $G(r)$ clearly reveals the presence of different medium-

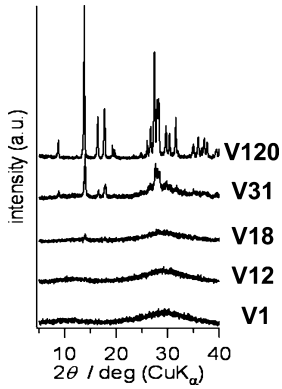

Figure 2. XRD patterns of the samples obtained by heating the zincosilicate solution for 1, 12, 18, 31, and 120 h (V1, V12, V18, V31, and V120, respectively). All Bragg peaks seen in the samples are due to VSV structure.

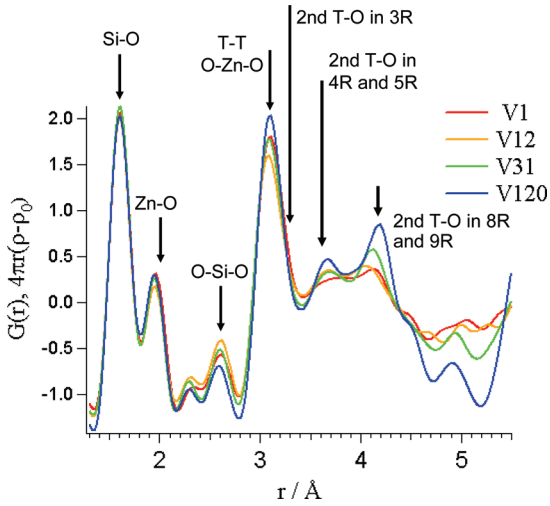

Figure 3. Pair distribution functions, $G(r)$, of the samples obtained by heating the zincosilicate solution for 1, 12, 31, and 120 h (V1, V12, V31, and V120, respectively). All assignments are derived from the crystal structure shown in Figure 1.

range orders in these systems. This indicates that the Zn-rich amorphous aluminosilicates have larger fractions of 3R and smaller fraction of other rings, compared with bulk silica (Si/Zn = ∞). This result supports the theory that the introduction of Zn atoms into silicate networks induces the formation of 3R in the amorphous solids.

Raman spectra of the samples are shown in Figure 6. It has been shown that bands in the 200−600 cm^{-1} region are sensitive to the T−O−T bond angle, the network connectivity, and the size of the ring systems present in the framework.[16–18,23–25] Previous Raman investigations on zeolite and silica assigned bands at ca. 370−430 cm^{-1} to 5R. Furthermore, Raman shifts at ca. 470−530 cm^{-1} and 550−600 cm^{-1} are associated with 4R and 3R. The band intensity of 5R (ca. 440 cm^{-1}) and 4R (ca. 490 cm^{-1}) increases relatively to 3R (ca. 600 cm^{-1}) as the synthesis progresses and finally four prominent bands (444 cm^{-1} (5R), 495 cm^{-1} (4R), 526 cm^{-1} (4R) and 591 cm^{-1} (3R)) are seen in V120 (Sprit bands in 4R is thought to be due to Zn−O−Si and Si−O−Si). This tendency is consistent with the HEXRD results shown in Figure 3. For comparison, the Raman spectra of amorphous aluminosilicate (i.e., at the initial stage of zeolite crystallization) for the synthesis of sodalite and ferrierite together with V1 are shown in Figure 7. Note that these zeolites do not contain 3R in the framework structure as shown in the Supporting Information. This shows that the

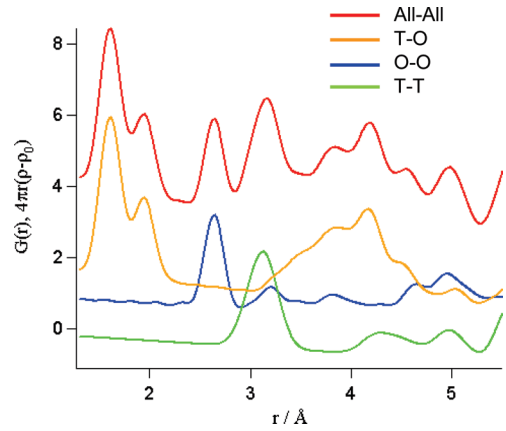

Figure 4. Calculated partial pair distribution function of VPI-7 (VSV type zeolite) by PDFgui. Top: $G(r)$ is shown for calculated crystalline VPI-7. Contributions of each relation are shown below. It is possible to understand the contribution of atomic relations for each peak of $G(r)$. For example, 3.1−4.3 Å is mainly due to the second nearest neighbor correlation to T−O in various rings. Note that the functions of O−O, T−O and All−All are shifted upwards by 1, 2 and 5, respectively, for clarity.

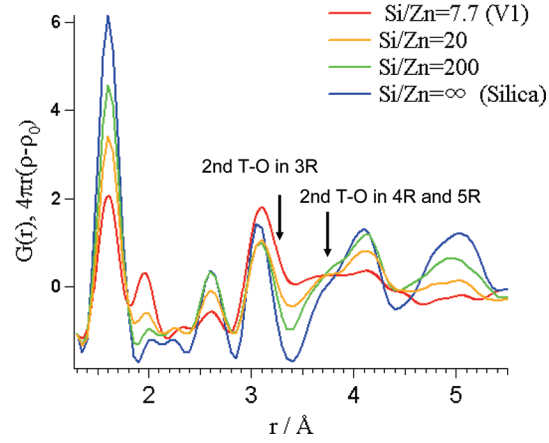

Figure 5. Pair distribution functions, $G(r)$, of the samples obtained by extracting the amorphous zincosilicate solids with the compositions of Si/Zn = 7.7 (V1), 20, and 200, together with bulk amorphous silica.

fraction of 3R formed in the amorphous zincosilicate is obviously larger than that in aluminosilicates which are used for the synthesis of sodalite and ferrierite, indicating that the introduction of zinc atom into silicate network induces the formation of 3R, while that of Al atoms do not. All these results demonstrate that the addition of Zn leads to the formation of 3R in the amorphous solids, which seems to be a key process in the crystallization of VPI-7. Furthermore, the difficulty in forming 3Rs in amorphous aluminosilicate at the initial stages of crystallization seems to be a reason for there only being a single example of aluminosilicate zeolites containing 3R (ZSM-18).

Conclusions

Changes in the medium-range order during crystallization of VPI-7 were characterized by a combination of HEXRD and Raman Spectroscopy. Clear changes are seen in the medium-range order, especially in the formation of 3R in the initial stages of crystallization of VPI-7, and increases in the proportion of other rings during crystallization has been confirmed. Addition of Zn seems to be required for the formation of 3Rs in the amorphous solids which, in turn, seems to be a key factor in

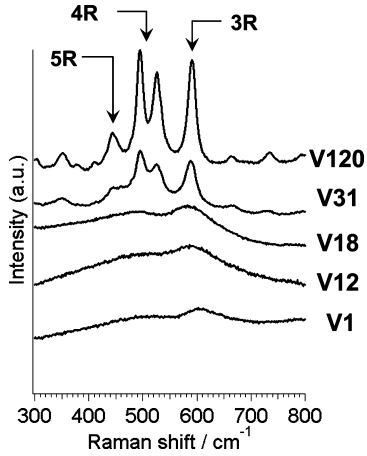

Figure 6. Raman spectra of the samples obtained by heating the zincosilicate solution for 1, 12, 18, 31, and 120 h (V1, V12, V18, V31, and V120, respectively). It has been shown that bands in the 200−600 cm^{-1} region are sensitive to the T−O−T bond angle, the network connectivity and the size of the ring systems present in the framework.

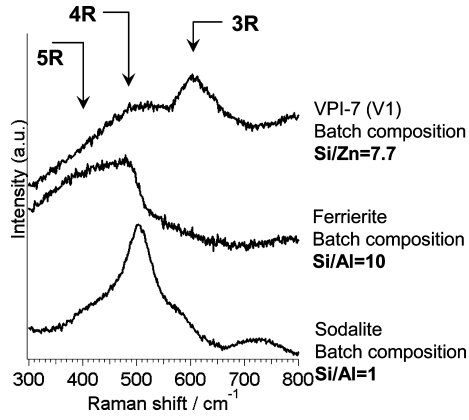

Figure 7. Raman spectra of V1 and amorphous aluminosilicates. Amorphous aluminosilicates were obtained prior to the crystallization of ferrierite (Batch composition Si/Al = 10) and sodalite (Batch composition Si/Al = 1), as shown in the Supporting Information.

the crystallization of zeolites containing 3Rs in their structure. Recently, various unique zeolites containing 3Rs in their structures, such as ITQ-33 and ITQ-44, have been reported,[26,27] and application of the present method to other zeolites is of interest. Furthermore, HEXRD in combination with reverse Monte Carlo modeling can provide us information on more accurate atomic arrangements of the precursor particles.[11] Work into these questions is now in progress and are likely to provide the structural pathway for the formation of microporous materials.

Acknowledgment. This work was financially supported by Giant-in-Aid for Scientific Research (JSPS). The X-ray diffraction experiment at the SPring-8 was approved by the Japan Synchrotron Radiation Research Institute under proposal No. 2005B0224.

Supporting Information Available: Preparation of amorphous zincosilicates with different compositions, preparation of amorphous aluminosilicates with different compositions, and the crystal structure of sodalite and ferrierite. This material is available free of charge via the Internet at http://pubs.acs.org.

References and Notes

(1) Davis, M. E.; Lobo, R. F. *Chem. Mater.* **1992**, *4*, 756.
(2) Cundy, C. S.; Cox, P. A. *Chem. Rev.* **2003**, *103*, 663.
(3) Wakihara, T.; Okubo, T. *Chem. Lett.* **2005**, *34*, 276.
(4) Kumar, S.; Wang, Z. P.; Penn, R. L.; Tsapatsis, M. *J. Am. Chem. Soc.* **2008**, *51*, 17284.
(5) Pelster, S. A.; Schüth, F.; Schrader, W. G. *Anal. Chem.* **2007**, *15*, 6005.
(6) Akporiaye, D. E.; Price, G. D. *Zeolites* **1989**, *9*, 23.
(7) Wood, I. G.; Price, G. D. *Zeolites* **1992**, *12*, 320.
(8) Many zeolite framework types can be analyzed by viewing them as layered structures, derived by the repetition, with stacking operators, of periodic, 2-D, 3-connected layers. Furthermore, the average number of polygon edges in a 2-D 3-connected net is six, that is, 6R; therefore, according to such zeolites, the introduction of smaller rings, such as 3R, is one of the ways to realize a zeolite structure with extra-large pores.
(9) Brunner, G. O.; Meier, W. M. *Nature* **1989**, *337*, 146.
(10) http://www.iza-structure.org/databases/.
(11) Annen, M. J.; Davis, M. E.; Higgins, J. B.; Schlenker, J. L. *Chem. Commum.* **1991**, 1175.
(12) Röhrig, D.; Gies, H.; Marler, B. *Zeolites* **1994**, *14*, 498.
(13) Wakihara, T.; Kohara, S.; Sankar, G.; Saito, S.; Sanchez-Sanchez, M.; Overweg, A. R.; Fan, W.; Ogura, M.; Okubo, T. *Phys. Chem. Chem. Phys.* **2006**, *8*, 224.
(14) Wakihara, T.; Suzuki, Y.; Fan, W.; Saito, S.; Kohara, S.; Sankar, G.; Sanchez-Sanchez, M.; Ogura, M.; Okubo, T. *J. Ceram. Soc. J.* **2009**, *117*, 277.
(15) Wakihara, T.; Yamakawa, T.; Tatami, J.; Komeya, K.; Meguro, T.; Kohara, S. *J. Am. Ceram. Soc.* **2007**, *90*, 1562.
(16) Yu, Y.; Xiong, G.; Li, C.; Xiao, F. S. *Microporous Mesoporous Mater.* **2001**, *46*, 23.
(17) Li, C.; Xiong, G.; Liu, J. K.; Ying, P. L.; Xin, Q.; Feng, Z. C. *J. Phys. Chem. B* **2001**, *105*, 2993.
(18) Dutta, P. K.; Shieh, D. C.; Puri, M. *J. Phys. Chem.* **1987**, *91*, 2332.
(19) Kohara, S.; Suzuya, K.; Takeuchi, K.; Loong, C. K.; Grimsditch, M.; Weber, J. K. R.; Tangeman, J. A.; Key, T. S. *Science* **2004**, *303*, 1649.
(20) Faber, T. E.; Ziman, J. M. *Philos. Mag.* **1965**, *11*, 153.
(21) Keen, D. A. *J. Appl. Cryst.* **2001**, *34*, 172.
(22) Farrow, C. L.; Juhás, P.; Liu, J. W.; Bryndin, D.; Božin, E. S.; Bloch, J.; Proffen, T. H.; Billinge, S. J. L. *J. Phys.: Condens. Mater.* **2007**, *19*, 335219.
(23) Pasquarello, A.; Car, R. *Phys. Rev. Lett.* **1998**, *80*, 5145.
(24) Annen, M. J.; Davis, M. E. *Microporous Mesoporous Mater.* **1993**, *1*, 57.
(25) de Man, A. J. M.; Ueda, S.; Annen, M. J.; Davis, M. E.; van Santen, R. A. *Zeolites* **1992**, *12*, 789.
(26) Corma, A.; Diaz-Cabanas, M. J.; Jorda, J. L.; Martinez, C.; Moliner, M. *Nature* **2006**, *443*, 842.
(27) Jiang, J.; Jorda, J. L.; Diaz-Cabanas, M. J.; Yu, J.; Corma, A. *Angew. Chem.* **2010**, *49*, 4986.

JP109373Z